Journal of Applied Electrochemistry **31**: 617–622, 2001.

Modelling of through-hole electrodeposition Part II: Experimental study

S.H. CHAN[1,2] and H.Y. CHEH[1,3]
[1]*Department of Chemical Engineering and Applied Chemistry, Columbia University, New York, NY 10027, USA*
[2]*Present address: Bristol-Myers Squibb Pharmaceutical Research Institute, New Brunswick, NJ 08903, USA*
[3]*Present address: Duracell, Berkshire Corporate Park, Bethel, CT 06801, USA*

Received 1 January 1999; accepted in revised form 21 November 2000

Key words: current distribution measurements, through-hole electrodeposition

Abstract

Current distribution measurements in through-hole electrodeposition were made on sectioned copper electrodes in a cylindrical flow channel. Two copper plating solutions with the same copper sulfate concentration but with different sulfuric acid concentrations were used. Experiments were conducted potentiostatically and under steady-state conditions. Results were compared with those from the theoretical model.

List of symbols

c_1	concentration of cupric ion (mol cm^{-3})
$c_{1\infty}$	bulk concentration of cupric ion (mol cm^{-3})
c_2, c_{H^+}	concentration of hydronium ion (mol cm^{-3})
c_3, $c_{SO_4^{2-}}$	concentration of the sulfate ion (mol cm^{-3})
c_4, $c_{HSO_4^-}$	concentration of the bisulfate ion (mol cm^{-3})
D_1, D_2, D_3, D_4	diffusion coefficient of cupric ion, hydronium ion, sulfate ion and bisulfate ion (cm^2 s^{-1}), respectively
E_{avg}	average error
E_{tot}	sum of the deviations between the experimental and the theoretical
I	current passing to each sectioned electrode (A)
F	Faradaic constant (96 487 C equiv^{-1})
i_{avg}	average current density (A cm^{-2})
i_0	exchange current density (A cm^{-2})
i	local current density (A cm^{-2})
i/i_{avg}	normalized local current density
$iR_0/(nFD_1c_{1\infty})$	dimensionless local current density
L_2	length of the through-hole (cm)
L	thickness of the ring electrode (cm)
n	number of electrons transferred
Pe	Peclet number $(2 < v_x > R_0)/D_1$
R_0	radius of the through-hole (cm)
R_1	outer radius of the ring electrode (cm)
r	ratio of the normality of the added ion to that of the counterion
T	temperature (K)

1. Introduction

Theoretical polarization curves and current distributions for through-hole electrodeposition have been computed for systems where effects due to ionic migration are important [1]. In this paper experimental data are gathered and compared with theoretical results. A copper solution of 0.01 M was chosen so that the thickness of the metal deposited on the surface of the working electrode is small compared to the radius of the through-hole. If higher concentrations were used, the metal deposited on the surface of the working electrode may be a significant fraction of the radius, leading to breakdown of the model. This would lead to a moving boundary problem so that the fluid mechanics and the mass transfer must be solved simultaneously for each time step to accurately predict the current distribution. Experimental conditions and parameters are carefully selected so that a comparison can be made between both theory [1] and experiment. Two different copper sulfate solutions with the same concentration of $CuSO_4$ (0.01 M) but different concentrations of H_2SO_4 (0.0667 and 0.0045 M) were used. A parameter, r, defined as the ratio of the normality of the hydronium ion to that of the sulfate ion, was used to characterize the electrolyte:

$$r = \frac{c_{H^+}}{2c_{SO_4^{2-}}} \tag{1}$$

The respective r values for the two electrolytes were 0.870 and 0.310.

2. Experimental system

The experimental set-up to determine the current distribution is shown schematically in Figure 1. The section of the acrylic tube (A), inner diameter 1.27 cm and length of 3.01 cm, served as the buttress where the back of the innermost ring electrode was seated. The remaining section of (A), inner diameter 1.905 cm and length of 4.03 cm, held 12 ring electrodes with Teflon washers (D) inserted between consecutive ring electrodes to prevent electrical contact between the ring electrodes. (A) was internally threaded at both ends to allow the connection of the threaded tube (B) whose length was 17.17 cm. This entrance region was sufficiently long so that a laminar flow was fully developed. Before (B) was connected to (A), a rubber O-ring was inserted to avoid leakage of the solution.

Counter electrodes (I1 and I2) were connected to (B) at both ends. Electrical contact to each section was made by placing brass screws through openings at the top of (A). A small capillary (H) with an inner diameter of 0.05 cm connected the electrolyte to the reference electrode compartment (G).

Experiments were performed on ring electrodes with an inner radius of 0.635 cm, an outer radius of 0.953 cm, and a thickness of 0.318 cm, as shown in Figure 2. The Teflon washer (D) had a thickness of 0.0253 cm. These dimensions correspond to a through-hole with an aspect ratio of 3.2.

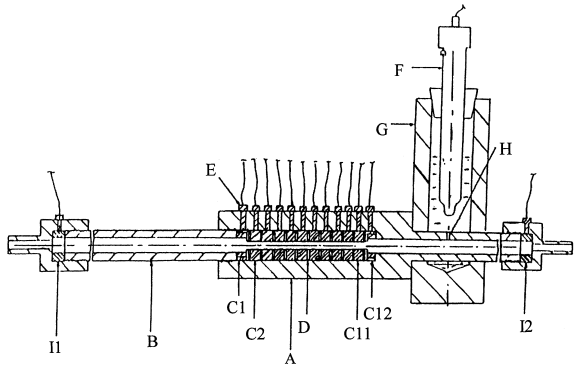

Fig. 1. Experimental model of the through-hole electrode system. Key: (A) acrylic tube, (B) threaded tube, (C) ring electrodes, (D) Teflon washer, (E) brass screws, (F) reference electrode, (G) reference electrode compartment, (H) capillary, and (I) counter electrode.

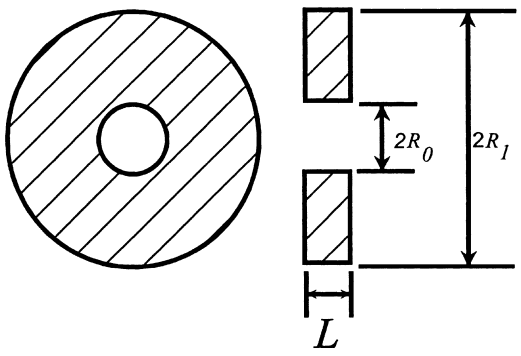

Fig. 2. A schematic diagram of a ring electrode. ($R_0 = 0.635$ cm, $R_1 = 0.935$ cm, $L = 0.318$ cm).

3. Experimental procedure

The inner radius of the ring electrodes was first polished with a 600 grit emery paper to remove copper oxide on the surface and then polished with a 200 grit emery paper until a mirror-like surface was obtained. Afterwards, the sides of these sections were mechanically polished with 0.20 μm wet alumina powder on a rotating grinder to obtain a flat, mirror-like finish and then rinsed with tap water.

All 12 sectioned electrodes were sonicated in a soap solution for at least 3 min and then rinsed with tap water to remove the remaining soap film. All sections were then cleaned with a cotton tip soaked in methanol, sonicated in methanol for 5 min, and rinsed again with tap water. The above procedure was repeated three times by replacing methanol with a 10% chromic acid solution, then with a 10% nitric acid solution, and finally with a 10% sulfuric acid solution. All sections were then dried with Kinwipes, cleaned with a cotton tip soaked in methanol to remove the last trace of inorganics, and cleaned with a dry, clean cotton tip before insertion into (A). Teflon washers (D) were placed between adjacent ring electrodes. The threaded tubes (B) were then connected to both ends of (A), separated in between by an O-ring. The counter electrode compartments (I) were connected to both ends of the threaded tubes. Tygon tubes were then connected to both ends of (I).

The solution from the reservoir was pumped by a Masterflex pump (Cole–Parmer, model N-07553-20) with a speed controller from the left to the right as shown in Figure 3. Initially, the flow channel was tilted 45° to remove all air bubbles. Once a steady flow rate was obtained, the flow channel was returned to its horizontal position.

The reference compartment (G) was filled entirely with the electrolyte before insertion of the standard calomel reference electrode (Fischer Scientific SCE). The solution flowing into the flow channel was pumped from the bottom of the reservoir to the top of the reservoir. Brass screws were inserted into the threaded holes of (A) to provide electrical contact. The current to the individual sections was obtained by measuring the potential difference across a 10 Ω precision shunt resistor with a digital multimeter (Keithly, model 177).

Solutions were prepared from distilled water filtered through a reverse osmosis water purification system (Mill-Q Reagent Water System), $CuSO_4 \cdot 5H_2O$ (Fischer certified ACS Reagent Grade), and H_2SO_4 (Fisher certified ACS Plus Reagent Grade). The solutions were then deareated by bubbling nitrogen gas through it for at least 30 min.

Immediately prior to electrolysis, the reading on the peristalic pump was set to the desired flow rate. The

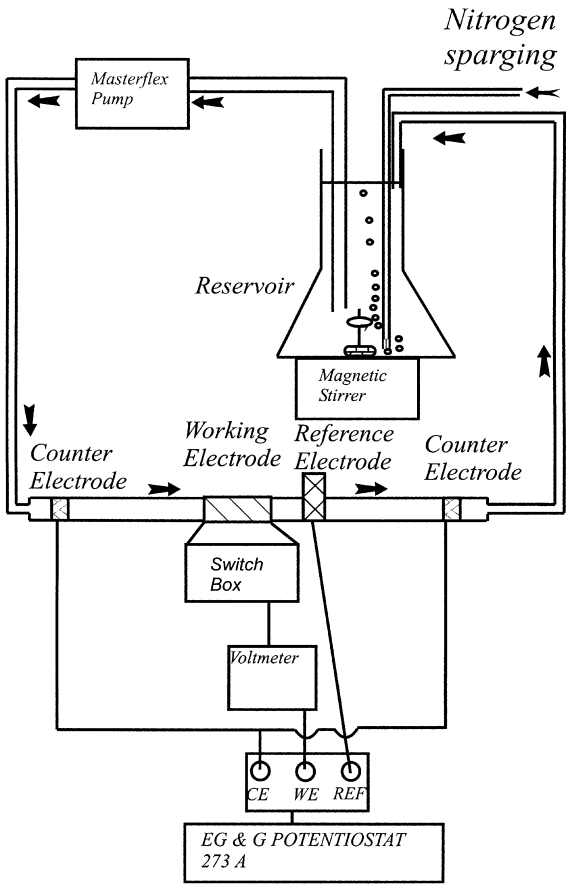

Fig. 3. Experimental apparatus.

actual flow rate was measured by collecting a specific liquid volume on a graduated cylinder and timed with a stop watch. The actual flow rate was then compared to the set flow rate to ensure that the proper reading was obtained.

All the experimental measurements were made using a potentiostat/galvanostat (PAR, model 273 A) at room temperature (22.0 ± 1 °C) and 1 atm. Before any data were recorded, a thin layer of copper was deposited on the surface of the sectioned electrodes at a current density of 0.05 mA cm^{-2} and at a flow rate of 120 ml min^{-1} for about 5 min. This corresponds to a copper thickness of approximately 0.35 μm.

4. Results and discussion

The mixed electrolyte is assumed to exhibit no interaction effects due to the low reactant concentration. A plot of the experimental limiting current against the volumetric flow rate and application of the Leveque solution [2] gave a value of the diffusion coefficient of the cupric ion as $0.635 \times 10^{-5}\,cm^2\,s^{-1}$. For the other ions, the diffusion coefficients at infinite dilution [2] were used for the simulation. By comparing the experimental and the theoretical current distributions (with $\alpha_a = 0.75$ and $\alpha_c = 0.25$), an exchange current density value of 0.001 A cm^{-2} gave the best fit. All the other kinetic parameters were taken from Mattson and Bockris [3], while the remaining parameters have been summarized previously [1].

Theoretical and experimental polarization curves are shown in Figures 4 and 5 under the assumption that cathodic potentials and currents are taken to be positive. The experimental polarization data were obtained using a potentiodynamic sweep rate of $10\,mV\,s^{-1}$ and recorded on an IBM PC through a data acquisition board. A comparison of the two figures indicates that the polarization curves corresponding to the less supporting electrolyte are ohmically dominated and are nearly linear over most of the regime. Although not shown, the experimental polarization data in Figure 5 continue to

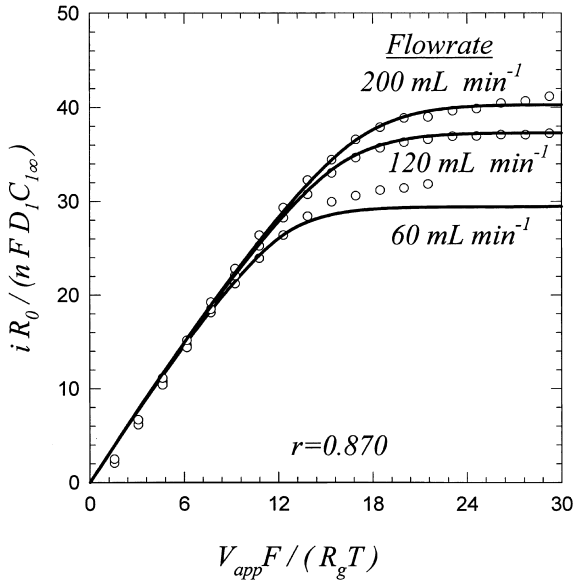

Fig. 4. Polarization curves. Key: (○) experimental and (——) theoretical.

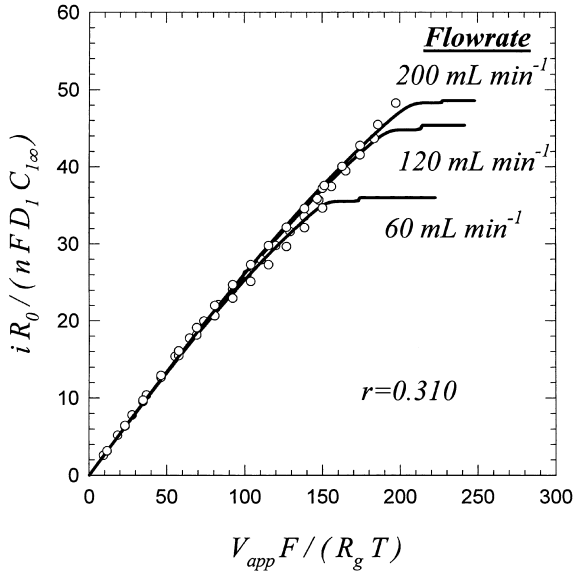

Fig. 5. Polarization curves. Key: (○) experimental and (——) theoretical.

increase monotonically and does not reach a limiting plateau as predicted by the model. As the applied potential is increased, a larger overpotential is exhibited at the entrance and possibly at the exit regions of the through-hole. Thus, secondary reactions such as the evolution of hydrogen and the hydrolysis the water starts to take place in these regions of the working electrode even before the cupric ion has reached zero concentration thereby leading to the masking of the limiting plateau. This is clearly one of the limitations of the model because it only considers the metal deposition reaction at the surface of the working electrode.

For flow rates of 120 and 200 ml min^{-1}, good agreement was found between the experimental and theoretical limiting current density, for $r = 0.87$. These volumetric flow rates correspond to Peclet numbers of approximately 3×10^5 and 5×10^5, respectively. A maximum deviation of 10% was found between the experimental and theoretical values of the limiting current density at a low flow rate of 60 ml min^{-1} corresponding to a Peclet number of 1.5×10^5. Since a peristaltic pump was used, fluctuations in the fluid flow may be a possible source of error. At low fractions of the limiting current, the current distribution is very uniform and exhibits a secondary-like profile. It is seen that the current distributions become more nonuniform at higher applied potentials. Mass transfer effects become more apparent at large fractions of the limiting current as shown in Figure 6 at 61.6% $i_{\lim}$ and in Figure 7 at 80% $i_{\lim}$. For current distributions near the limiting current, the current density is highest at the entrance of the through-hole and decreases downstream. At the limiting current, the diffusion layer is the thinnest at the entrance and continues to grow along the electrode. Figures 8 and 9 show the current distributions to be less uniform than Figures 6 and 7 due to the lower conductivity of the solution. At higher current densities, Figures 8 and 9 both show numerical results exhibiting a local maximum near the right side of the working electrode. Possible explanations leading to deviations between theory and experiment is that the model does not consider any secondary reactions occurring on the electrode such as hydrogen evolution. To measure experimentally the local maximum for this geometry, more sectioned electrodes must be constructed and placed in the right side of the working electrode. In all cases, satisfactory agreement was found between the experiment and the theory.

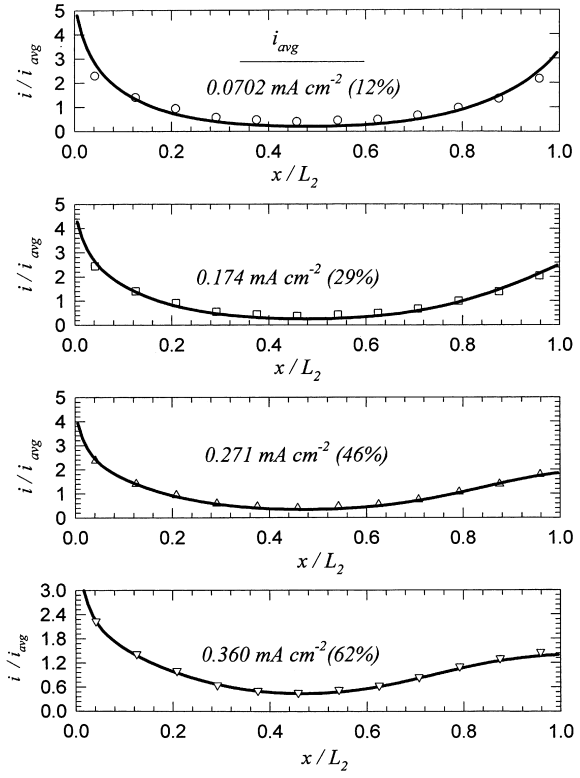

Fig. 6. Current distribution at 60 ml min^{-1} ($r = 0.870$). Value in parenthesis refers to the percent of the limiting current.

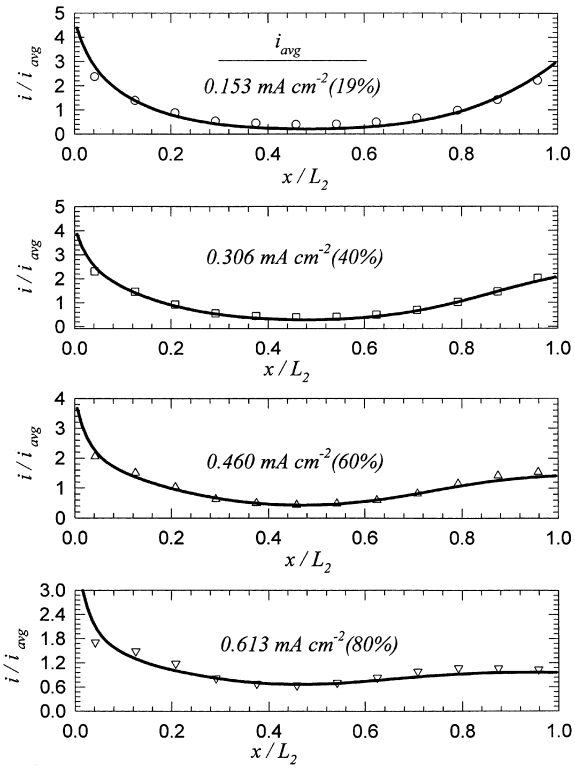

Fig. 7. Current distribution at 120 ml min^{-1} ($r = 0.870$). Value in parenthesis refers to the percent of the limiting current.

For a sectioned electrode system, we define an average error, E_{avg}, by

$$E_{\text{avg}} = \frac{E_{\text{tot}}}{N} \tag{2}$$

where N is the number of sections. E_{tot} is the sum of the deviations between the theoretical and experimental current passing to each electrode given by,

$$E_{\text{tot}} = \sum_{j=1}^{N} \left\| \frac{I_{\text{theor}(j)} - I_{\text{expt}}(j)}{I_{\text{expt}}(j)} \right\| \tag{3}$$

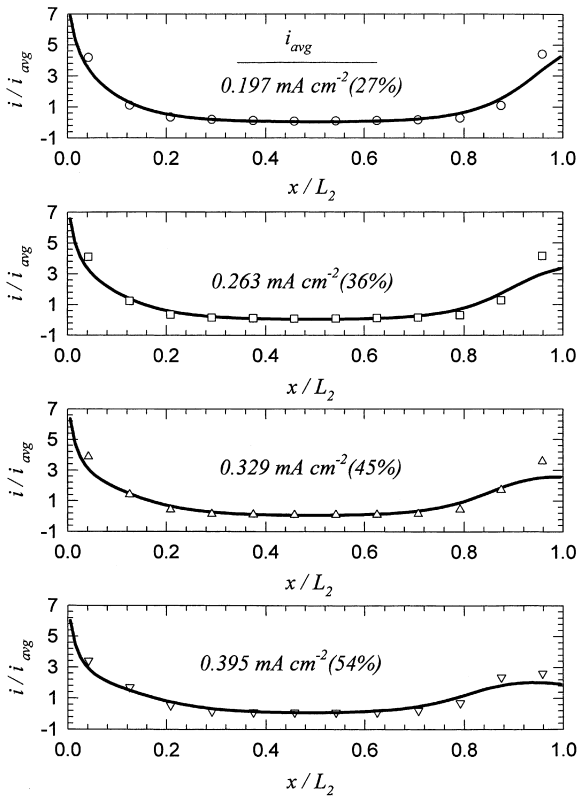

Fig. 8. Current distribution at 60 ml min^{-1} ($r = 0.310$). Value in parenthesis refers to the percent of the limiting current.

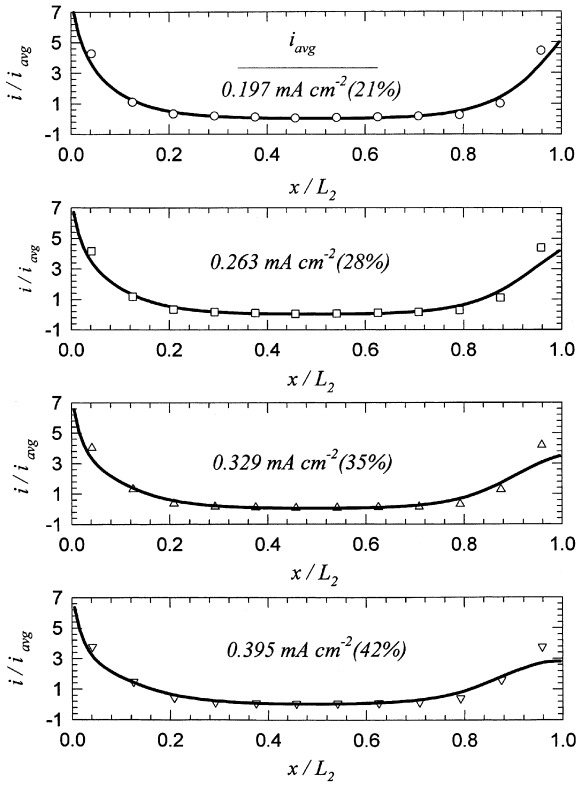

Fig. 9. Current distribution at 120 ml min^{-1} ($r = 0.310$). Value in parenthesis refers to the percent of the limiting current

Table 1. Parameters used in the simulation

$\alpha_a = 0.75$
$\alpha_c = 0.25$
$n = 2$
$i_0 = 0.001\,\mathrm{A\,cm^{-2}}$
$D_1 = 0.635 \times 10^{-5}\,\mathrm{cm^2\,s^{-1}}$
$D_2 = 9.312 \times 10^{-5}\,\mathrm{cm^2\,s^{-1}}$
$D_3 = 1.063 \times 10^{-5}\,\mathrm{cm^2\,s^{-1}}$
$D_4 = 1.33 \times 10^{-5}\,\mathrm{cm^2\,s^{-1}}$
$v = 1.00 \times 10^{-2}\,\mathrm{cm^2\,s^{-1}}$

where $I_{\mathrm{theor}}(j)$ is the theoretical current passing to the jth electrode and $I_{\mathrm{expt}}(j)$ is the experimentally measured current passing to the jth electrode. $I(j)$ is defined by

$$I(j) = 2\pi R_0 \int_{x_j}^{x_j+\Delta x_j} i(x)\,\mathrm{d}x \tag{4}$$

where R_0 is the radius of the through-hole, $i(x)$ is the local current density at position x, and Δx_1 is the thickness of the jth electrode. The average current density, i_{avg}, was calculated by the summation of the total current passing through all of the individual electrodes divided by the electrode surface area exposed to the electrolyte:

$$i_{\mathrm{avg}} = \frac{\sum_{j=1}^{N} I(j)}{2\pi R_0 L_2} \tag{5}$$

where L_2 is the length of the through-hole.

Table 1 is a summary of the average error calculated from the different experimental conditions. In most cases, a slightly higher average error was calculated as the current density was increased. Better agreements between the theory and the experiment occurred at

Table 2. Summary of the average error

Flow rate /ml min^{-1}	i_{avg} /mA cm^{-2}	E_{avg} /%
Summary of the average error, E_{avg}, for $r = 0.874$:		
60	0.07019	14.4
60	0.1743	5.7
60	0.271	2.2
60	0.359	7.5
120	0.153	4.4
120	0.306	5.3
120	0.459	7.8
120	0.613	6.3
Summary of the average error, E_{avg}, for $r = 0.310$:		
60	0.197	3.5
60	0.263	6.2
60	0.329	8.3
60	0.395	9.3
120	0.197	5.0
120	0.263	6.8
120	0.329	8.5
120	0.395	11.5

lower current densities where kinetic effects were more significant. At higher current densities, there is less agreement between theory and experiment because the model neglects any secondary reactions such as the evolution of hydrogen occurring at the working electrode. With the assumptions embedded in the theoretical model, this is definitely the expected trend between both theory and experiment.

5. Conclusions

Experimental polarization and current distribution measurements were made for two different copper sulfate solutions with the same concentration of $CuSO_4$ (0.01 M) but different concentrations of H_2SO_4 (0.0667 and 0.0045 M). These experiments were all performed at flow rates corresponding to Peclet numbers ranging from 1.5×10^5 to 5×10^5. Satisfactory agreement was found between theory and experiment with the maximum average error on current distribution to be less than 15%. Possible sources of deviation is that the model does not consider any secondary reactions such as the hydrolysis and the evolution of hydrogen. One of the assumptions of the model is no consideration of the role of the bisulfate ions. Improvements in the experimental design such as having more sectioned electrodes in the local maximum regions is important to accurately measure the current distribution.

References

1. S.H. Chan and H.Y. Cheh, *J. Appl. Electrochem.*, submitted.
2. J.S. Newman, 'Electrochemical Systems', 2nd edn (Prentice Hall, New Jersey, 1991).
3. E. Mattson and J.O'M. Bockris, *Trans. Faraday Soc.* **55** (1959) 1986.
4. J.E. Chern and H.Y. Cheh, *J. Electrochem. Soc.* **143** (1996) 3139.
5. A.M. Pesco and H.Y. Cheh, *J. Electrochem. Soc.* **135** (1989) 399.